



## Modeling of Air-Water Filled Rubber Dam Under Hydrostatic Conditions

Qusay S. Khaleel<sup>\*</sup>, Thair S. Khayyun , Khudhayer N. Abdullah

Civil Engineering Dept., University of Technology-Iraq, Alsina'a street, 10066 Baghdad, Iraq.

\*Corresponding author Email: <mailto:42370@student.uotechnology.edu.iq>

### HIGHLIGHTS

- The simulations achieved a very low error rate compared to the experimental findings as the membrane tension increased the upstream head increased.
- The dam height rises as the upstream head rises with all cases of internal pressure.

### ABSTRACT

Inflatable dams, also called rubber dams, are flexible cylindrical inflatable and deflatable structures attached to a rigid base; these dams are basically cylindrical tubes made of rubberized material and inflated by air, water, or a combination of the two. In this paper, the air/water inflatable dam was studied and analyzed numerically using ANSYS software. The 3-parameter Mooney-Rivlin Model was used to model the rubber material of the dam. At first, a physical model from literature was used to calibrate the results of the ANSYS software, and then a new model was analyzed with different dimensions and conditions. Thirty-six simulations were made using the ANSYS software to calibrate the software, based on experimental results from the literature. The simulations achieved a very low error rate compared to the experimental findings, with a maximum error rate of 1.45 percent. After that, a new air/water-filled dam model simulation was carried out. The new inflatable dam was analyzed with large dimensions that can be used to reserve water at high elevations. Several water heights (2, 4, 6, 8, and 10 m) were used as input at the upstream of the dam, and their effect on the dam body was verified on the assumption that there was no water downstream of the dam for all simulations. The height of the used inflatable dam was assumed to be 11 meters (first 5.5 m water pressure and the second 5.5m different air pressure values), and the bottom gaskets was 9.7 meters wide. It is evident from the analysis that the upstream water appears to push the dam to the right side (towards downstream), causing a change in dam equilibrium shape. The difference in the cross-sectional equilibrium profile of the dam is due to the change in air and water pressures on the element. Thus, it changes the tension and slope of the dam membrane elements. The simulation results showed that the membrane tension increases as the upstream head increases, and as the internal pressure increases, the tension increases. This rise in tension as the upstream head rises may be due to the rise in the forces on the element, and hence the membrane tension increases.

### ARTICLE INFO

**Handling editor:** Wasan I. Khalil

**Keywords:**

Rubber Dam  
Numerical simulation  
Ansys software  
Mooney-Rivlin models

## 1. Introduction

The rubber dam is a highly efficient water control structure that greatly outperforms the traditional steel gate systems. It consists of a high tensile elastic rubber-coated fabric bladder, always fixed on a reinforced concrete foundation. Air, water, or both (air/water) inflates the bladder, which reserves and controls the flow of water and is decreased by the release of air or water from the inside of the bladder. The inflatable dam is a relatively new type of gate, which allows for savings in capital expenditure and maintenance costs Michael [1]. Michael et al. [2] compared between steel gates and an inflatable dam and reached a set of benefits for the inflatable dams such as:

1. The design is simple with no movable parts such as hinges or bearings; no corrosion or sealing issues, or lubricants that can damage the environment, are involved. As a result, settlements or earthquakes do not impact inflatable dams.
2. There is no need for drive mechanisms, such as hydraulic cylinders, electric actuators, or chains, which require significant maintenance. Inflatable dams are operated by injecting or deflating air or water.
3. The inflatable dams can be operated safely and can always be deflated to prevent clogging. In addition, dam membranes can be installed or changed in a few weeks so that construction, inspection, and regeneration times are greatly reduced.

Inflatable dams have been studied experimentally and theoretically by some researchers in the literature. El- Jumaily and Salih [3] studied air-inflated and water-inflated dams' behavior under hydrostatic conditions. The study was conducted using a physical model, and it was analyzed under various internal pressure values and various upstream and downstream water heads. The experimental data obtained are compared with theoretical results obtained by using computer software describing profiles of the dam, the height of the dam, and the cross-sectional area of the dam. Maurer et al.[4] simulated the inflatable dams partially filled with water and gas using FEM, taking into account large deformations and stability of the dam. The deformation-dependent loading concerning the stability of the effect of the internal pressure of gas and water filling can be calculated directly. Michael[1] investigated experimentally and theoretically the inflatable rubber dam. The theoretical part has done based on FEM by using the ABAQUS software. Gurt[5] presented actual calculation methods and design aspects of the inflatable rubber dams.

The basic of the numerical simulations is that instead of designing and building a physical model using expensive devices such as a Data Logger, Doppler Velocity Meter, Ultrasonic Flowmeter, Water Pressure Sensors... etc. Instead, the behavior of fluids such as velocity distribution, turbulence kinetic energy, stress-strain relationships, pressure distribution... etc., can be obtained through Computational Fluid Dynamics (CFD) software such as Ansys Workbench FLOW3D, and COMSOL Multiphysics ®... etc. This computer software is developed to solve and analyze the fluid behavior and solid materials behavior by solving the partial differential equations based on the conservation of mass, energy, conservation of momentum, etc. By using this computer software, the user can get an “actual feel” of the defined problem. This is an attractive idea for solving complex problems and large model studies for which there is no need for extra workers or an existing large setup to determine the actual results.

The 2D behavior of the inflatable rubber dams concerning the boundary conditions of the dam was numerically simulated in this paper. The study aims to simulate an inflatable rubber dam that can be used to reserve water with high head elevations. To achieve the study's objectives, the ANSYS software was used to perform the simulations and verify the results using experimental data from the literature.

## 2. Geometry

A specific shape is used to study the water pressure on the dam's wall. First, the solid dam geometry is drawn utilizing Solid works, 2018 software Lombard [6]. Next, the geometry used in the simulations is exported as a Parasolid (x-t) file format, which could be read by Static structural. The (x-t) files are then directly imported into static structural where the appropriate mesh can be generated. The height of the used inflatable dam was assumed to be 11 meters (first 5.5 m water pressure and the second 5.5m different air pressure values), and the bottom gaskets were 9.7 meters wide. The geometric representation of the dam model to simulate the static pressure is shown in Figure 1. The thickness of the inflatable rubber dam is designed according to Alpha Rubber &Plastic Co., Ltd. Figure 2 illustrates the relationship between the height of the rubber dam and its membrane thickness.

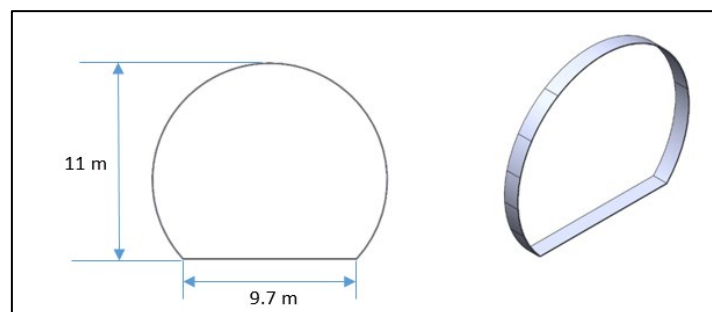


**Figure 1:** Numerical model geometry of dam to simulate the static pressure (Solid Works, 2018).

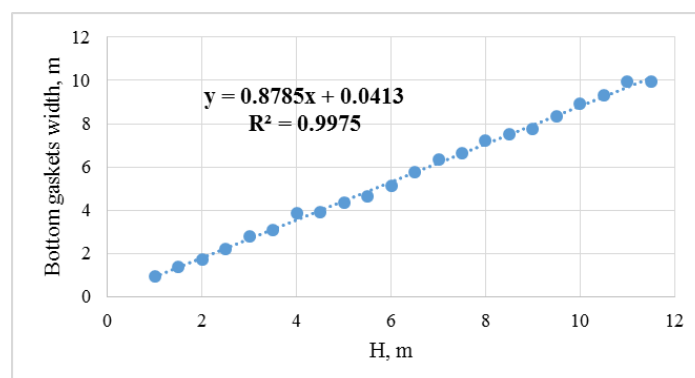


**Figure 2:** Relationship between the height of the rubber dam and bottom gaskets width (Alpha Rubber & Plastic Company).

### 3. Mesh Domain

Mesh generation is the most important issue for an accurate solution. If the good quality of the mesh is generated, one can obtain realistic results from the numerical model. A crucial aspect of any numerical simulation is deciding the required grid domain and a suitable mesh cell dimension. Both the precision of the results and the simulation time can be influenced by mesh and cell dimensions, so it is necessary to reduce cell dimensions while including adequate resolution to catch the important geometry characteristics and sufficient flow details. Starting with relatively large cell dimensions and then increasingly reducing the mesh size until the output no longer varies dramatically with any more reductions is an efficient way to evaluate the crucial cell dimensions. Assigning too many cells will prolong the progression of the computation. The increasing number of cells increases the computation time as each cell's calculations are carried out. The optimum number of cells should, therefore, be allocated.

This study used hexahedral element type in the rubber dam simulation, as shown in Figure 3. The hexahedral element is modeled with 6 degrees of freedom (3 translations and 3 rotations). Figures 4 illustrate the mesh of the dam model in the Ansys static structure.

The mesh considering one of the affecting factors in the simulation process. Therefore, different cell sizes are selected to identify the best cell size that satisfies the phenomenon conditions. To obtain the accurate solution, about 4030 elements were used in Ansys static structural and 656290 elements in Ansys fluent. Table 1 represents the validation of the mesh element size used in the rubber dam simulation. It shows that element size 0.1m is the best because there is a slight difference in deformation for smaller elements size after this value. So, it no needs to refine the mesh more because this will increase the solution time.

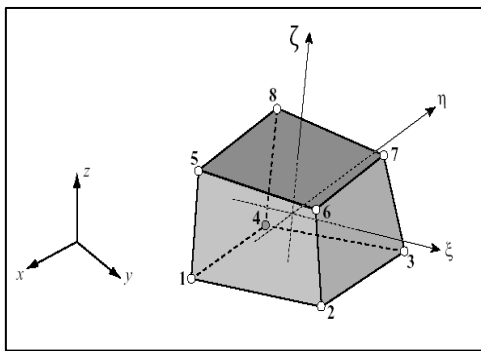


Figure 3: Hexahedral used mesh (Ansys 18.2).

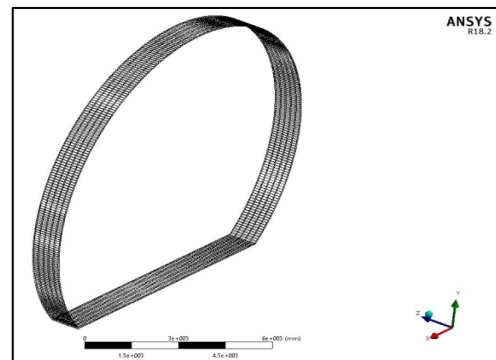


Figure 4: Mesh in Ansys static structural (Ansys 18.2).

Table 1: The validation of the mesh element size (m).

Mesh size(m)	0.5	0.4	0.3	0.2	0.1	0.05	0.04
No. of elements	336	630	1096	2040	4030	24900	50150
Max. Deformation	2.164	2.173	2.175	2.185	2.191	2.195	2.197
	3	4	2	8	5	1	1

### 4. Boundary Conditions of Ansys static structural

One of the most critical steps of numerical flow simulation is identifying the necessary boundary conditions. The boundary conditions must match the physical conditions of the problem correctly. Ansys Static structural utilizes the hexahedral orthogonal mesh in the Cartesian coordinates to describe the 3-dimensional deformation. Therefore, six boundaries are specified on the rectangular mesh prism—the boundary conditions used by this study as shown in Figures 5 and 6.

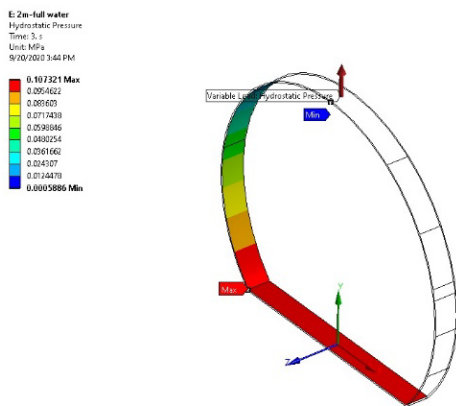


Figure 5: Hydrostatic pressure effect on the internal wall of the rubber dam, fixed base, and no displacement in the Z direction.

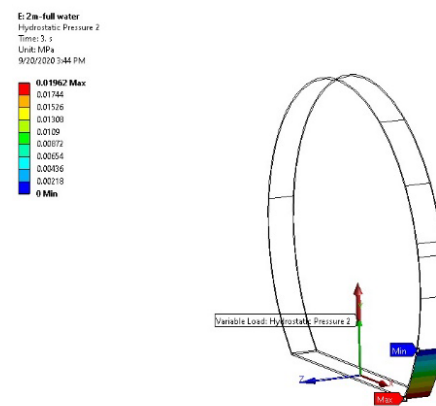


Figure 6: Hydrostatic pressure effect on the external wall of the rubber dam, fixed base, and no displacement in the Z direction.

### 5. Material Properties

In any numerical simulation, the properties of fluids like temperature, viscosity, and density shall be defined as input. The fluid is chosen from the software database, and its properties are defined on the fluids tab. Ansys software contains a library of popular materials to assist users. Hyper-elasticity material is used in this study for analyzing the rubber-like materials (elastomers). In a wide range of structural applications, rubber-like materials distinguished by a comparatively low elastic modulus and a high bulk modulus are utilized. These materials are generally called 'hyper-elastic material' and are encountered with large elastic strains and deformations with minimal volume change (almost incompressible material). Suppose an elastic strain energy density function (W) is a scalar function of strain deformation tensors. In that case, a material is said to be hyper-elastic, the derivatives of which specify the necessary strain components concerning the corresponding stress components. Therefore, both material nonlinearity and substantial deformation occur within hyper-elastic constitutive models. A representative hyper-elastic structure (a balloon seal) is shown in Figure 7.

The behavior of hyperplastic materials means that these materials behave or respond elastically to large strains and do not deform plastically. Various material models are available to model the hyperplastic material. Some of the available hyper-elastic models are Neo-Hookean (working at 30% shear strain), Mooney-Rivlin (working at 30% in compression and 200% in tension relying on order), Arruda-Boyce (working at 300% shear strain), and Ogden (working up to 700% shear strain) [7]. The Mooney-Rivlin Material Model (MRMM) was used to model the rubber material of the dam. This model requires the stress-strain test data collected from previous literature work.

In this analysis, because the elastic effect is prevalent relative to the visco-elastic one, the solid propellant is assumed to be an incompressible hyper-elastic solid. The stress condition of the hyper-elastic material is calculated by taking the strain energy density derivatives concerning the components of the strain.

One of the popular models of the phenomenological form is the model of Mooney Rivlin. for a particular strain, the stress state is calculated in relation to the strain components as the derivatives of the stress-energy density. The function of the strain-energy density is:

$$W = W(\bar{I}_1, \bar{I}_2, J) \tag{1}$$

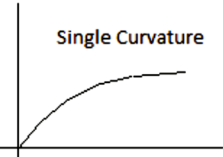
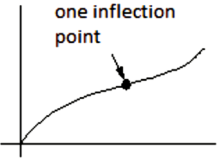
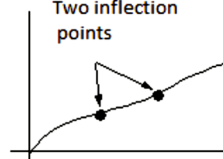
The Second Piola-Kirchhoff stress is given as follows:

$$\bar{S} = \frac{\partial W(\bar{I}_1, \bar{I}_2)}{\partial E} \tag{2}$$

Where: W is the strain energy function,  $\bar{I}_1$ = first deviatoric strain invariant,  $\bar{I}_2$ = second deviatoric strain invariant, J=determinant of the elastic deformation gradient, and  $\bar{S}$ ,  $\partial E$ , are the components of the second Piola-Kirchhoff stress tensor (s), the Green- Lagrange strain tensor (E), respectively.

The Mooney-Rivlin model is available in the literature to explain the hyperelastic material behavior as a function of strain invariants with various parameters, such as two, three, five, and nine parameter models. The Mooney Rivlin models with 2 and 3 parameters have no inflection point (single curvature), and the 5-parameter model has one inflection point (double curvature). In contrast, the 9-parameter model has two inflection points. In this study, 3- parameters Mooney Rivlin model were used. The appropriate model type may be chosen based on the stress-strain curve [7], as shown in Table 2.

**Table 2:** Suitable Mooney Rivlin model [7].

Strain-Stress Curve	Suitable Mooney-Rivlin Model
 <p>Single Curvature</p> <p>No inflection point (single curvature)</p>	2 or 3 parameters
 <p>one inflection point</p> <p>One inflection point (double curvature)</p>	5 parameters
 <p>Two inflection points</p> <p>Two inflection points</p>	9 parameters

The Mooney-Rivlin hyper-elastic constitutive model's strain energy function is expressed as a function of the  $I_1, I_2, I_3 = J^2$  strain invariants. The type of strain energy density function for Mooney-Rivlin models of 3- parameters is given as:

$$W_{(3)} = C_{10}(\bar{I}_1 - 1) + C_{01}(\bar{I}_2 - 1) + C_{11}(\bar{I}_1 - 1)(\bar{I}_2 - 1) + \frac{1}{d}(J - 1)^2 \tag{3}$$

Where d = material incompressibility parameter.

For the incompressible Mooney-Rivlin model of 3 parameters, the corresponding uniaxial stress is given as in [7]:

$$\bar{S}_{3p} = 2C_{10} \left( \lambda - \frac{1}{\lambda} \right) + 2C_{01} \left( 1 - \frac{1}{\lambda^3} \right) + 6C_{11} \left( \lambda^2 - \lambda - 1 + \frac{1}{\lambda^2} + \frac{1}{\lambda^3} - \frac{1}{\lambda^4} \right) \tag{4}$$

To achieve the true behavior of the rubber material, the Mooney Rivlin model should satisfy the stability criterion. Where the stability criterion is given as follows:

$$\frac{\partial \sigma_{ij}}{\partial \varepsilon_{ij}} \geq 0 \text{ and } \partial \sigma_{ij} \partial \varepsilon_{ij} \geq 0 \tag{5}$$

Where:  $\lambda$ = deviatoric principal stretches,  $\partial \varepsilon_{ij}$ = the infinitesimal change in the logarithmic strain of material.

$\partial \sigma_{ij}$ = the change in Cauchy stress for defining the state of stress at a point inside a material in the deformed state.

Some constraints on the 3 parameters Mooney-Rivlin were given by the condition mentioned above, as mentioned below:

$$C_{10} + C_{01} \geq 0 \text{ and } C_{11} \geq 0 \tag{6}$$

Where  $C_{10}, C_{01}$ , and  $C_{11}$  are material constants characterizing the deviatoric deformation of the material.

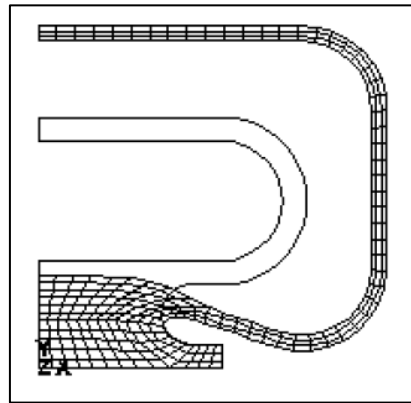


Figure 7: Hyper-elastic Structure (Ansys workbench 18.2)

### 6. Forces Acting on the Dam

The forces that are taken into consideration in this study (for hydrostatic pressure only) are the hydrostatic pressure (inside the dam and on the upstream side of the dam only with zero head downstream for all cases) as shown in Figure 8, and the membrane material weight of 1500 kg/m<sup>3</sup> according to ASTM D790 standard [8]. The membrane thickness is designed according to the specifications of Alpha Rubber & Plastic Co., Ltd. Figure 7 illustrates the relationship between the height of the rubber dam and the bottom gaskets width of the dam.

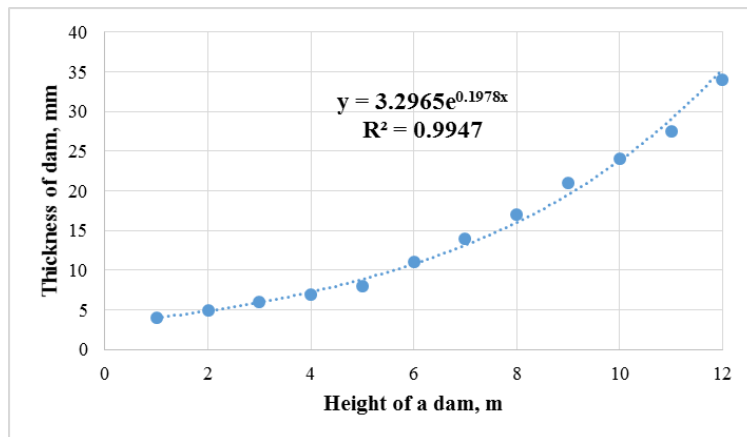


Figure 8: Relationship between the height of rubber dam and its thickness

### 7. Filling Conditions

The filling state defines the structure's response to the load conditions. In this study, the behavior of a mixture of air and water inflated dams is numerically analyzed under various conditions of internal air pressures and upstream heads of water. The internal water pressure was assumed to fill half of the dam (Constant at 5.5m), while the internal air pressure was used with three values of 9 m, 10 m, and 11 m. Figure9 illustrates the filling conditions used in this paper.

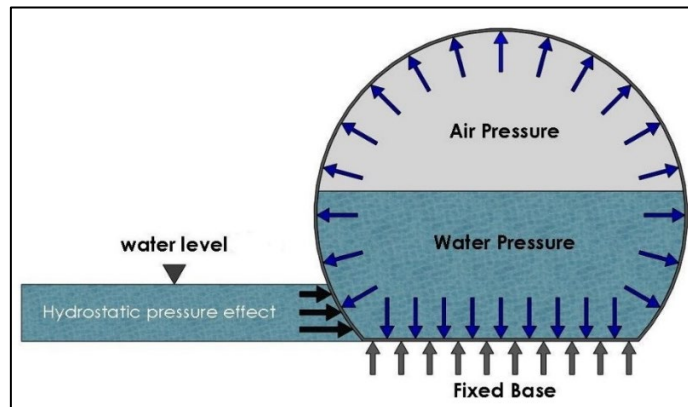


Figure 9: Forces acting on Air/Water-filled dam in this study.

### 8. Results and Discussion

To verify the results of the ANSYS software in simulating the inflatable rubber dams, a physical model was used from the literature. The model parameters used in the inflatable rubber dam simulation must first be set to verify the ANSYS software results. A model studied by El-Jumaily, and Salih [3] was used to calibrate and validate the results of ANSYS software. El-Jumaily and Salih [3] analyzed the performance of the Inflatable rubber dams under hydrostatic conditions experimentally. Experiments have been conducted to analyze the inflatable dam using water and air as a filling material inside the dam bag. For the construction of the models, a rubber material with the properties described in Table 3 is used. Two models of dams, the air inflating dam and the water inflating dam, was constructed from a rectangular rubber layer of a 55.3 cm perimeter length, 0.1 cm thick membrane, and 15 cm base length.

Where 36 simulations were rendered using the ANSYS software, the findings were compared to El-Jumaily and Salih's experimental results [3]. Figure 10 demonstrates the stress-strain curve of the rubber dam material used by El-Jumaily and Salih [3]. Figures 11 and 12 compare dam height's experimental and numerical variation with an upstream head for various air and water pressures, respectively. The simulations achieved a very low error rate compared to the experimental findings, with a maximum error rate of 1.45 percent.

After calibration and verification of ANSYS software results based on the laboratory results from the literature, a new air/water-filled dam model simulation was carried out. The height of the new inflatable dam was assumed to be 11 meters (first 5.5 m water pressure and the second 5.5m different air pressure values), and the bottom gaskets were 9.7 meters calculated, as shown in Figure 2. Several water heights (2, 4, 6, 8, and 10m) were used as input at the upstream of the dam, and their effect on the dam body was verified on the assumption that there was no water downstream of the dam for all simulations.

To simulate the new inflatable dam model using the dimensions shown in Figure (1-a), high-tension rubber material with a thickness of 29 mm was calculated according to the relationship shown in Figure. Figure 13 demonstrates the stress-strain curve of the high-tension rubber material used by Lobo and Croop [9].

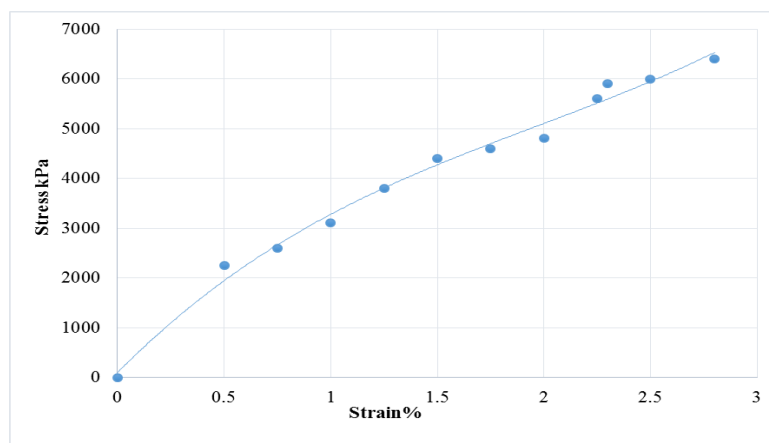
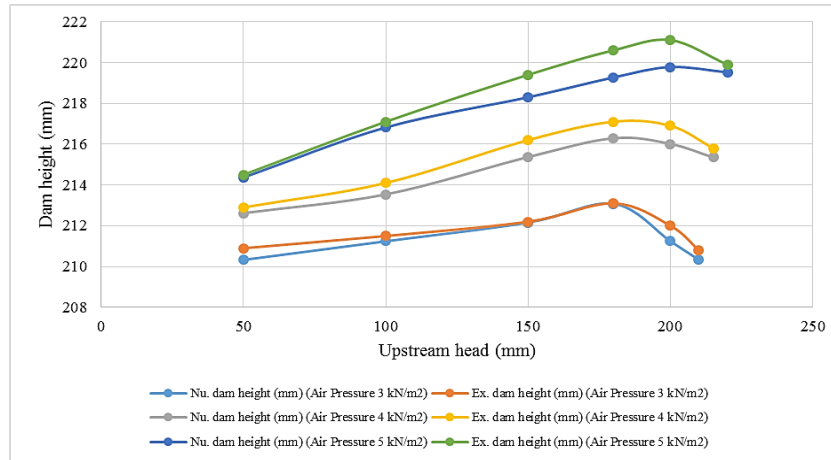


Figure 10: Stress-strain curve of the rubber dam material used by El-Jumaily and Salih [3]

**Table 3:** Rubber dam membrane properties [3]

Material	Thickness (cm)	Weight (kg/m <sup>2</sup> )	Tensile Strength (kN/m)
<b>Rubber</b>	0.1	1.3	6.453



**Figure 11:** Comparison between the experimental [3] and numerical variation of the dam height with a rising upstream head for different air pressures.

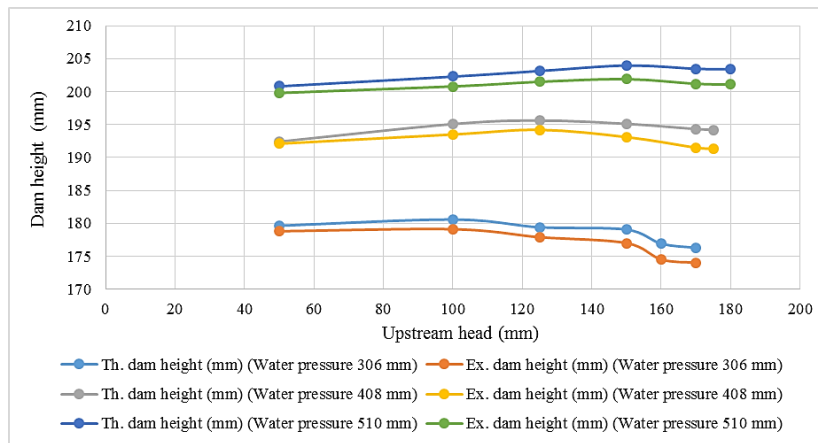


**Figure 12:** Comparison between the experimental [3] and numerical variation of the dam height with a rising upstream head for different water pressures.

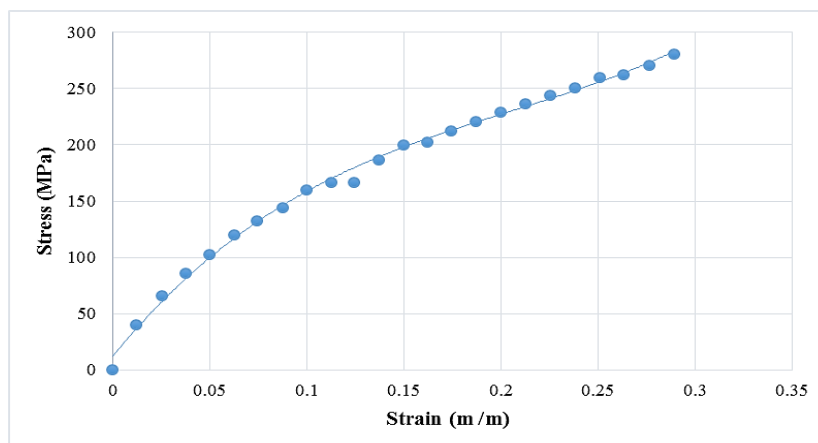


**Figure 13:** Stress-strain curve of the high-tension rubber material used (Lobo and Croop, 2016).

After entering the experimental data in Figure 13, the ANSYS software generates a fitting curve for the entered experimental data, as shown in Figure 14. The calibrated ( $C_{10}$ ,  $C_{01}$ , and  $C_{11}$ ) constraints values of the 3-parameters Mooney-Rivlin model by ANSYS software are shown in Figure 15.

Figures 16, 17, and 18 illustrate the effect of the upstream water pressure on the Cross-sectional equilibrium shapes of the dam at (5.5 m internal water pressure) and 9 m, 10m, and 11m internal air pressure, respectively. It is evident from these Figures that the exterior water appears to push the dam to the right side (towards downstream). The difference in the cross-

sectional equilibrium profile of the dam is due to the change in air and water pressures on the element. Thus, it induces a change in tension and slope of the dam membrane elements. In the event of a decrease in the internal air pressure, significant deformation of the equilibrium profile is observed. Figure 19 indicates a rise in the dam height as the internal air pressure is raised for the constant upstream head. Figure 20 shows that the dam height rises as the upstream head rises with all cases of internal pressure. This behavior will not persist reliant on internal pressure. For example, the dam height reaches a peak value of 11.91 m when the internal air pressure is raised to 11 m, and the upstream head is equivalent to 8 m and falls to 11.89 m when the upstream head is elevated to 10 m. It is evident from Figure 21 that due to the deformation towards the downstream side, the upstream slope (the angle between the horizontal foundation (bottom gaskets) and the slope of the first element on the inflatable dam's upstream face is the upstream slope of the dam) decreases as the upstream head rises. Figure 22 shows that as the upstream head rises with all internal air pressure values, the downstream slope (The angle between the horizontal foundation (bottom gaskets) and the last element's slope is the downstream slope of the dam) decreases.

The tension average between the upstream and downstream fixtures was computed using a user-defined function (UDF) in ANSYS. Figure 23 shows that the membrane tension increases as the upstream head increases, and as the internal pressure increases, the tension increases. This rise in tension as the upstream head rises may be attributed to the rise in the forces on the element, and hence the membrane tension increases. Around the same time, as the internal pressure is reduced, the internal components of air and the water forces decrease, allowing the membrane tension to decrease.

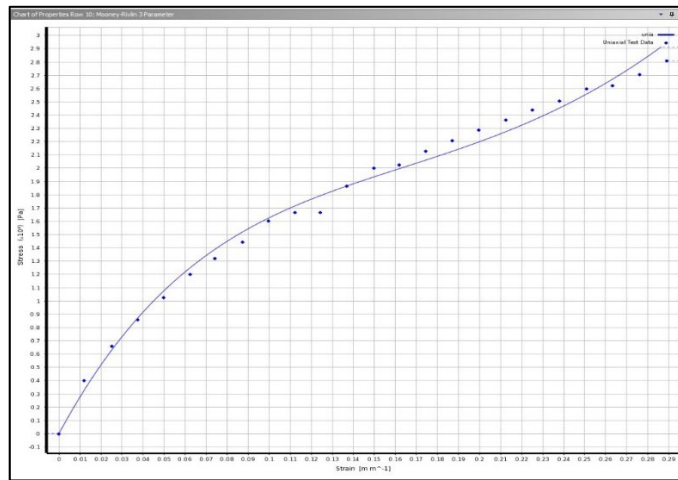
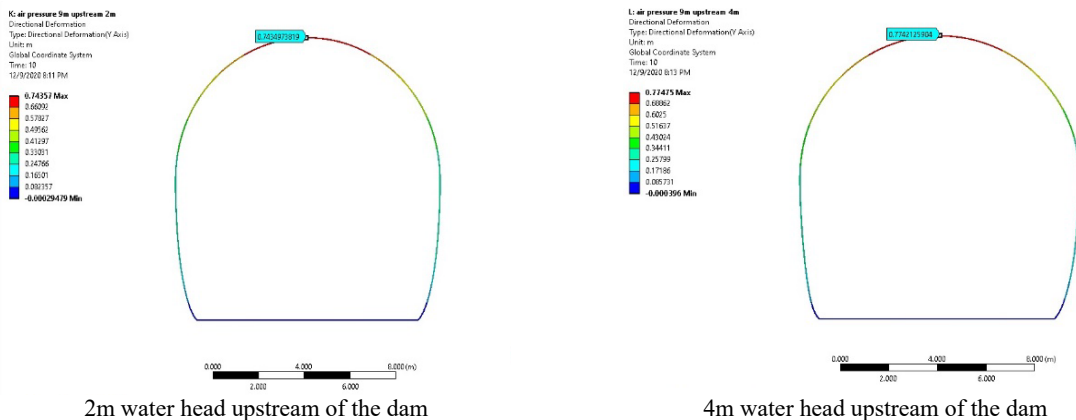


Figure 14: Mooney-Rilivn 3 parameters solve curve fitting by Ansys.

	B	C	D
1	Coefficient Name	Calculated Value	Calculated Unit
2	Incompressibility Parameter D1	0	Pa <sup>-1</sup>
3	Material Constant C01	2651449334	Pa
4	Material Constant C10	-2161095728	Pa
5	Material Constant C11	922308848.8	Pa
6	Residual	0.06567715136	
*			

Figure 15: The calibrated ( $C_{10}$ ,  $C_{01}$ , and  $C_{11}$ ) constraints values.



2m water head upstream of the dam

4m water head upstream of the dam



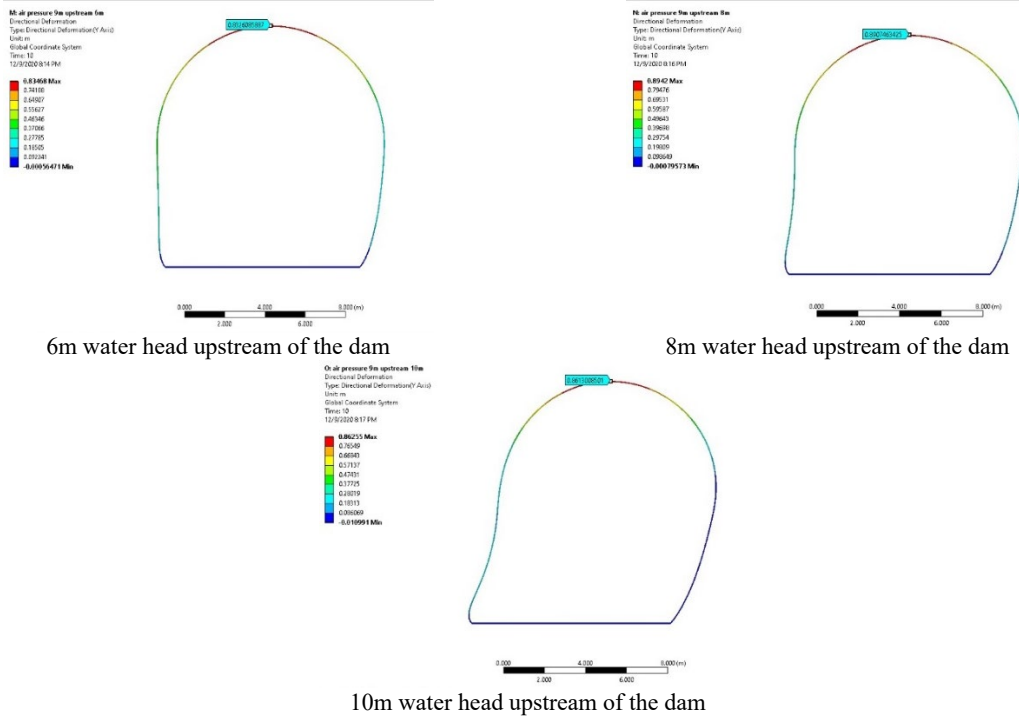


Figure 16: The dam's cross-sectional equilibrium shapes at 5.5 m internal water pressure and 9 m internal air pressure

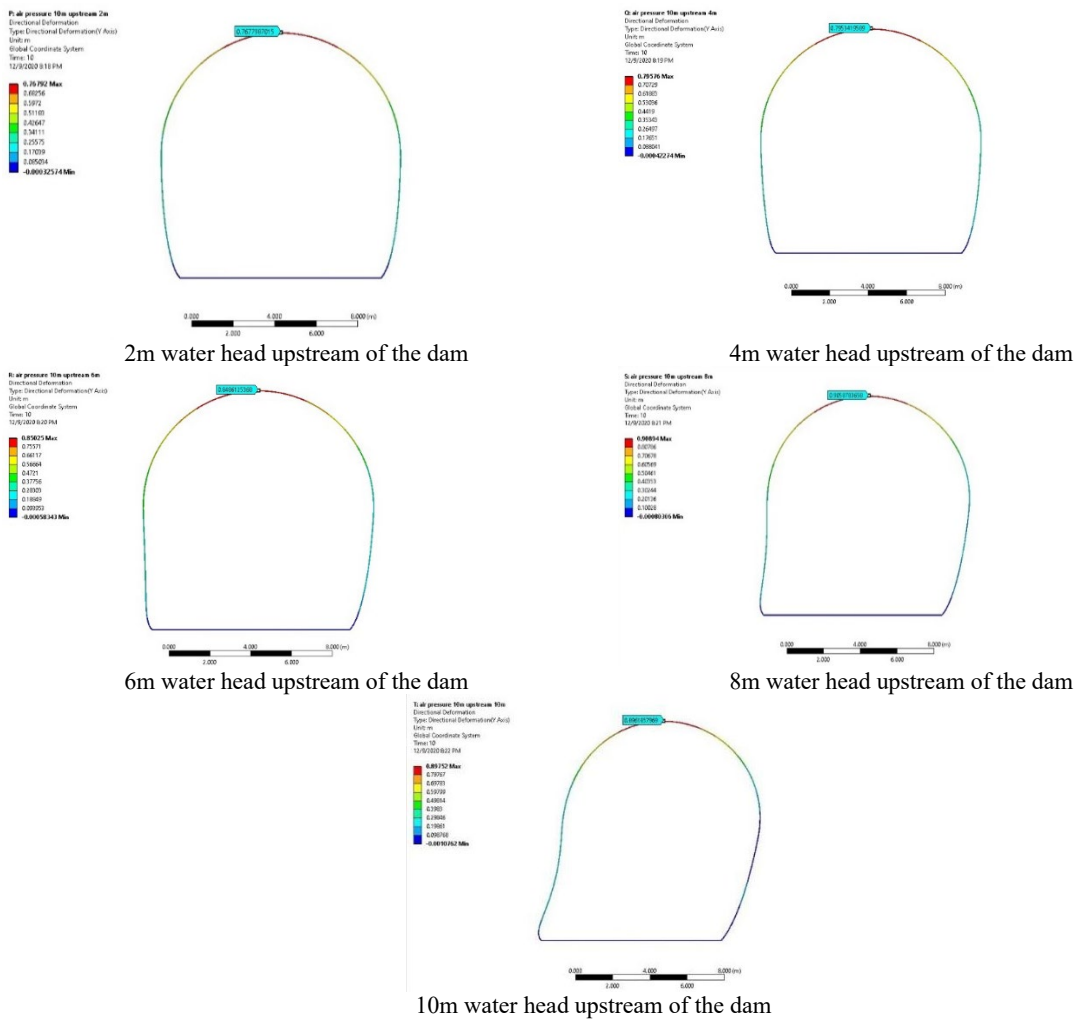


Figure 17: Cross-sectional equilibrium shapes of the dam at 5.5 m water pressure and 10 m internal air pressure.

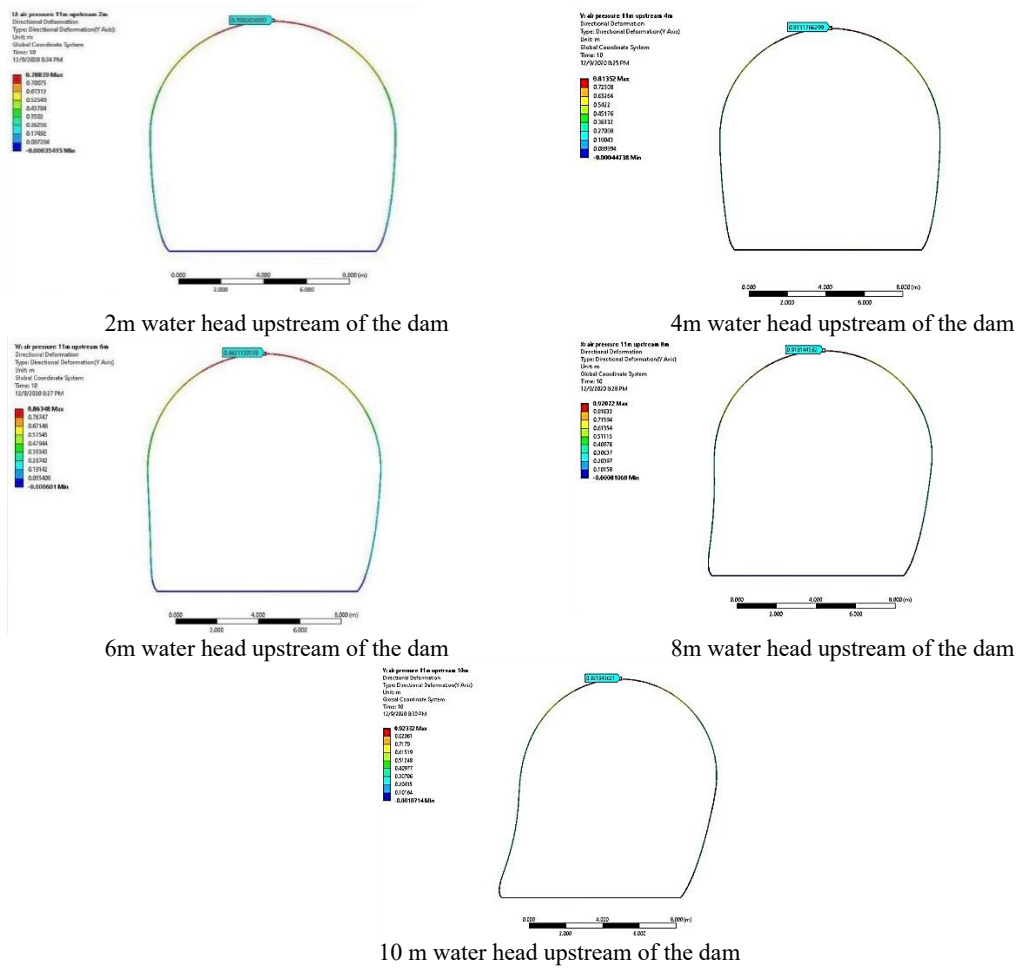


Figure 18: Cross-sectional equilibrium shapes of the dam at 5.5 m water pressure and 11 m internal air pressure.

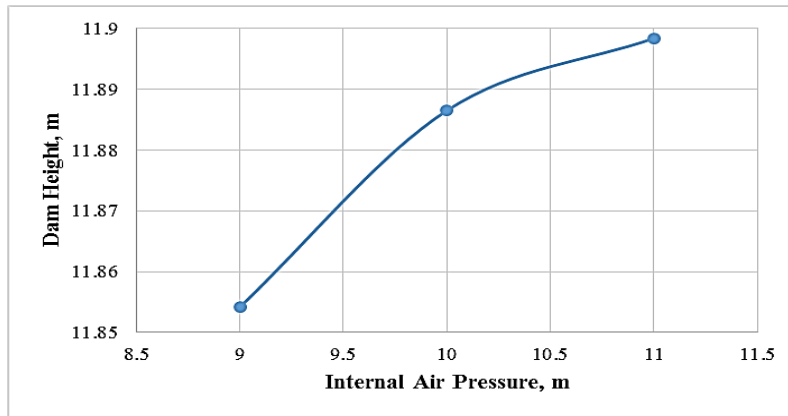


Figure 19: Variation of Dam height with increasing internal air pressure for constant upstream head.

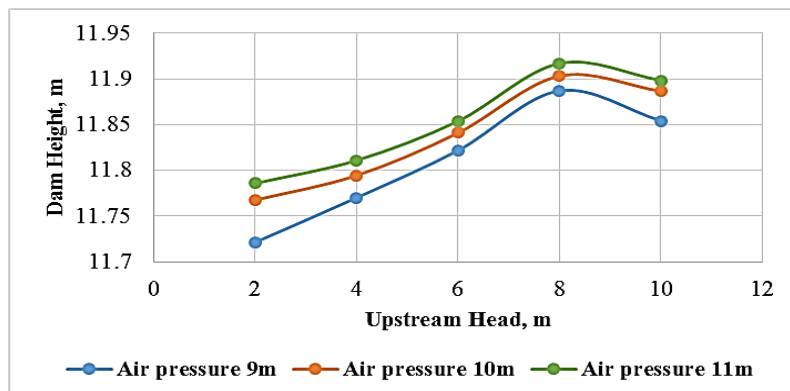


Figure 20: Variation of dam height with a rising upstream head for different air pressures.

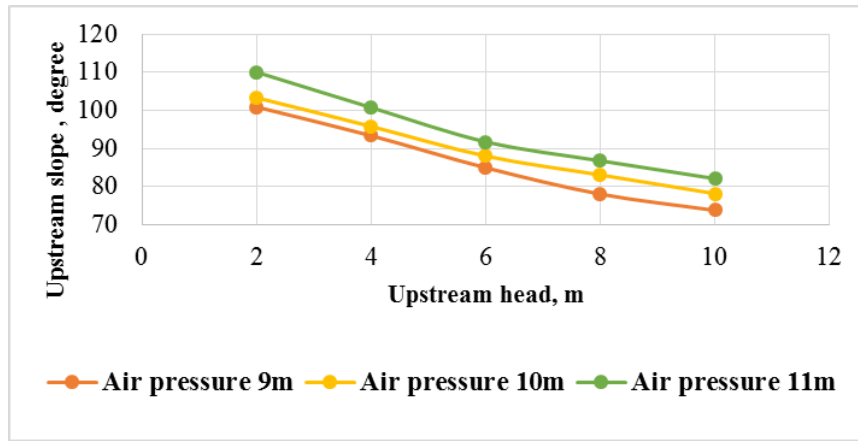


Figure 21: Variation of Upstream membrane slope with a rising upstream head for different air pressures.

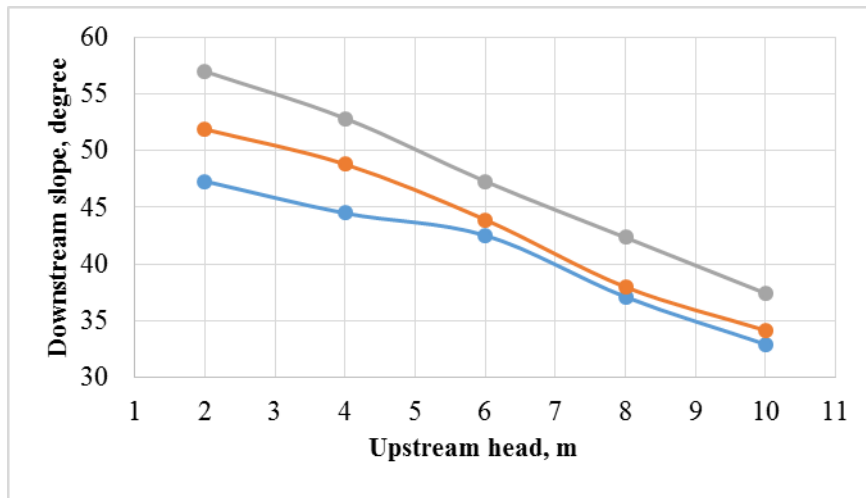


Figure 22: Variation of downstream membrane slope with a rising upstream head for different air pressures.

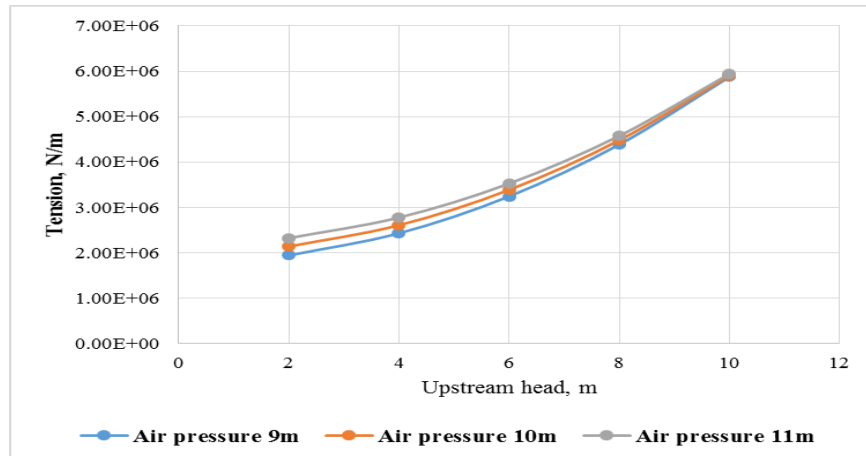


Figure 23: Difference of membrane tension with a rising upstream head for different air pressures

### 9. Conclusions

The ANSYS software was used to analyze inflatable rubber dams, where a physical model from the literature was first used to calibrate and validate the results of the ANSYS software. Then a new model was analyzed with different dimensions and different conditions. Finally, the 3-parameter Mooney-Rivlin Model was used to model the rubber material of the dam. Where 36 simulations were rendered using the ANSYS software, the findings were compared to the experimental findings performed [3]. The simulations achieved a very low error rate compared to the experimental findings, with a maximum error rate of 1.45 percent. After calibration and verification of ANSYS software results based on the laboratory results from the literature, a new air/water-filled dam model simulation was carried out.

The new inflatable dam was analyzed with large dimensions that can be used to reserve water at high elevations. It is evident from the analysis that the upstream water tends to push the dam to the right side (towards downstream), causing a change in dam equilibrium shape. The difference in the cross-sectional equilibrium profile of the dam is due to the change in air and water pressures on the element, which, thus, induces a change in tension and slope of the dam membrane elements. The simulation results showed a rise in the dam height as the internal air pressure is raised for a constant upstream head, and the upstream and downstream slopes decrease as the upstream head rises. Also, the results showed that the dam height rises as the upstream head rises with all cases of internal pressure. Therefore, this behavior will not persist reliant on internal pressure.

The simulation results showed that the membrane tension increases as the upstream head increases, and as the internal pressure increases, the tension increases. This rise in tension as the upstream head rises may be attributed to the increased forces on the element. Hence, the membrane tension increases.

#### **Author contribution**

All authors contributed equally to this work.

#### **Funding**

This research received no specific grant from any funding agency in the public, commercial, or not-for-profit sectors.

#### **Data availability statement**

The data that support the findings of this study are available on request from the corresponding author.

#### **Conflicts of interest**

The authors declare that there is no conflict of interest.

## **References**

- [1] G. Michael, On the hydraulic and structural design of fluid and gas filled inflatable dams to control water flow in rivers. In: E. Oñate, B. Kröplin and K.-U.Bletzinger (Hg.),5th Conference on Textile Composites and Inflatable Structures., Barcelona, Spain, 2011.
- [2] G. Michael, M. Maisner, and G. Ulrike, Inflatable dams - Prospects for the use of flexible gates Advantages and application range - Hydraulic and structural design - Requirements for materials - Initial experience on Federal waterways, 31st PIANC CONGRESS., 2006.
- [3] K. K., El-Jumaily, and A. A Salih, Analysis of inflatable dams under hydrostatic conditions, Int. j. eng ., 2005.
- [4] A. Maurer, M.Hassler, and K. Schweizerhof, Modeling of inflatable dams partially filled with fluid and gas considering large deformations and stability, International Conference on Textile Composites and Inflatable Structures, Structural Membranes, Barcelona, Spain,2009.
- [5] R. Gurt, Design and analysis of reinforced rubber membranes for inflatable dams,proceedings of the 7th International Conference on Textile Composites and Inflatable Structures, Barcelona, Spain, 2015.
- [6] M. Lombard, Mastering SolidWorks, John Wiley Sons, 1st ed.,Australia, 2018.
- [7] T.Saussman, and Bathe R.S., A Finite Element Formulation for Nonlinear Elastic and inelastic, Analysis, Comput, Struct., 26(1987) 357- 409 . [https://doi.org/10.1016/0045-7949\(87\)90265-3](https://doi.org/10.1016/0045-7949(87)90265-3)
- [8] Standard test methods for flexural properties of unreinforced and reinforced plastics and electrical insulating materials, ASTM D790, ASTM Standards, 1997.
- [9] H. Lobo, President, and B. Croop, Testing, Modeling, and Validation for Rubber Simulation in ANSYS,presented at the short course prepared for the Western Pennsylvania ANSYS User's Group Fall Workshop, Canonsburg, USA, 2016.
- [10] SolidWorks, Solid Works 2018 user manual.
- [11] Ansys Software18.2, Ansys workbench18.2user manual.
- [12] Alpha Rubber & Plastic Company.